

FLOW AND HEAT TRANSFER CHARACTERISTICS THROUGH A U-BEND

N.A. Kotb, I.M.El-Moghazy, A.A. Hegazy and M.A.Mahmoud

Mechanical Power and Energy Department, Faculty of Engineering,
Minia University, El-Minia, Egypt

ABSTRACT

Flow and heat transfer characteristics through a U-bend are investigated in this paper. The complete governing differential equations are solved numerically using two turbulent models, the standard $k-\epsilon$ model and the near-wall $k-\epsilon$ model, (present model). The present numerical results have been tested and evaluated against published experimental data. The present results indicate the advantage of the present model over the standard $k-\epsilon$ model of turbulence. Theoretical investigation has been done to study the effect of Reynolds number and curvature ratio upon Nusselt number. This study showed that Nusselt number increases with increasing Reynolds number and decreasing the curvature ratio in the curved portion and continue through the downstream tangent.

Keywords: U-bend; Curvature ratio, Turbulent flow; $k-\epsilon$ model; Connective heat transfer

INTRODUCTION

Turbulent convecting flows are widely encountered in thermofluid equipment, where the working characteristics and operating efficiencies are influenced by the nature of the given flow. These flows are habitually made to change direction and streamline curvature, such as those in passage between turbine and compressor blades, pipe bends in heat exchangers and cooling passages inside heated system components. The hydrodynamic nature of flow in the straight and curved ducts was outlined by Johnston [1]. Many experimental investigations for curved flow were motivated by specific design requirements of associated fluid equipment, such as Mayle *et al.* [2] and Enayet *et al.* [3]. On the other hand some of the experimental studies have been done to provide data for modeling purpose, for example Taylor *et al.* [4] and Humphrey *et al.* [5].

Turbulent flow through a curved channel with 90° bend was studied theoretically by Ktob *et al.* [6]. They showed that in sharp bends flow separation occurs on both inner and outer walls of the bend. Also, Metzger

and Larson [7] showed that the average heat transfer through a 90° bend increases to about 120% of its entrance value.

Turbulent convecting flow in a square duct with 180° bend was studied experimentally and numerically by Johnson [8, 9]. He carried out this study at a Reynolds number of 55,800 and a curvature ratio of 3.357, and constant wall heat flux. He pointed out that no separation of flow occurred at this curvature ratio. The predicted results by both algebraic stress model of turbulence and $k-\epsilon$ turbulence model were compared with experimental data. This comparison showed that a fair agreement was obtained especially for pressure coefficient and temperature distribution while a reasonable agreement for Nusselt number was achieved. Recently, Hedlund and Lagrani [10] reported an experimental investigation for heat transfer in a curved and straight channels with transitional flow. They showed that the important increases in Nusselt number occur due to a variety of laminar-to-turbulent transitional phenomena which occur mostly in the upstream straight portion of the

channel but then continue to cause important variations in the downstream curved portion. Also, for laminar and transient flow through curved or helical coiled ducts and channels, there were an enhancement in the heat transfer rate accompanied with a higher pressure drop, [11-14].

Recently, So *et al.* [15] compared between ten near-wall two-equation models for turbulent flow through parallel plates based on the direct numerical simulation and available experimental data. This comparison showed that the SAYS model is the best for the region near the wall. Thus this model is applied in the present study.

The work described in this paper is motivated for testing a flow simulation scheme against a set of convective heat transfer data. The near-wall two equation $k-\varepsilon$ model is compared with the standard $k-\varepsilon$ model which is commonly applied to turbulent flow. This comparison is evaluated using the experimental data for air flow and heat transfer through a U-bend given by Johnson [8]. Also, a theoretical study for predicting the effect of Reynolds number and curvature ratio on heat transfer and pressure drop is made.

GOVERNING EQUATIONS

The governing equations to be considered are the continuity, momentum, and energy equations. The flow was treated as a two-dimensional turbulent flow. Therefore, the mathematical model is based on the time-averaged equation. In the present study, the near wall $k-\varepsilon$ model was adopted. These equations were solved in Cartesian coordinates in the duct tangents, and Cylindrical coordinates were employed in the bend. The equations in Cylindrical coordinates are given by Johnson [8] while, for simplicity, they are written in the Cartesian coordinate system with tensor notation in the following form:

Continuity Conservation

$$\frac{\partial}{\partial x_j}(\rho u_j) = 0 \tag{1}$$

Momentum Conservation

$$\frac{\partial}{\partial x_j}(\rho u_j u_i) = -\frac{\partial p}{\partial x_i} + \frac{\partial}{\partial x_j}(\mu_{eff} \frac{\partial u_i}{\partial x_j}) \tag{2}$$

Energy Conservation

$$\frac{\partial}{\partial x_j}(\rho u_j T) = \frac{\partial}{\partial x_j}(\Gamma_{T,eff} \frac{\partial T}{\partial x_j}) \tag{3}$$

Turbulence

$$\frac{\partial}{\partial x_j}(\rho u_j k) = \frac{\partial}{\partial x_j}(\Gamma_{k,eff} \frac{\partial k}{\partial x_j}) + G - \rho \varepsilon \tag{4}$$

$$\frac{\partial}{\partial x_j}(\rho u_j \varepsilon) = \frac{\partial}{\partial x_j}(\Gamma_{\varepsilon,eff} \frac{\partial \varepsilon}{\partial x_j}) + C_{\varepsilon 1} \frac{\varepsilon}{k} G - C_{\varepsilon 2} \frac{\rho \varepsilon \varepsilon}{k} + \zeta \tag{5}$$

where $\mu_{eff} = \mu + \mu_t$ and

$$\Gamma_{T,eff} = \mu + \mu_t / \sigma_t, \quad \Gamma_{k,eff} = \mu + \mu_t / \sigma_k,$$

$$\Gamma_{\varepsilon,eff} = \mu + \mu_t / \sigma_\varepsilon,$$

The turbulent viscosity, μ_t , is obtained from;

$$\mu_t = C_\mu f_\mu \rho \frac{k^2}{\varepsilon} \tag{6}$$

The term G in Equations 4 and 5 represents the generation of turbulence energy given by

$$G = \mu_t \frac{\partial u_i}{\partial x_j} (\frac{\partial u_i}{\partial x_j} + \frac{\partial u_j}{\partial x_i}) \tag{7}$$

The damping function, f_μ , and the near-wall correcting function, ζ , are given as follows, [15];

$$f_\mu = (1 + \frac{3.45}{\sqrt{Re_t}}) \tanh(\frac{y^+}{115}) \tag{8}$$

$$\zeta = \exp[-(\frac{Re_t}{40})^2] [-0.57 \frac{\varepsilon \varepsilon}{k} + 0.5 \frac{(\varepsilon^*)^2}{k} - 2.25 \frac{\varepsilon}{k} G] \tag{9}$$

The reduced dissipation rates ε and ε^* are given by;

$$\tilde{\varepsilon} = \varepsilon - 2\nu(\partial\sqrt{k}/\partial y)^2$$

and

$$\varepsilon^* = \varepsilon - 2\nu k / y^2 \tag{10}$$

The turbulent Reynolds number is defined as:

$$Re_t = k^2 / \nu \varepsilon \tag{11}$$

The values specified for the model constants are given as follows:

$$C_\mu = 0.096, \quad C_{\varepsilon 1} = 1.5, \quad C_{\varepsilon 2} = 1.83, \\ \sigma_k = 1.0, \quad \sigma_\varepsilon = 1.45, \quad \sigma_t = 1.0$$

In addition to the above differential equations, the physical properties (c_p , μ , ρ , and λ) are given as functions of the fluid temperature, in the Appendix.

Solution of the Governing Equations

The computer codes used in the present study for the numerical solution of the governing equations belong to the TEACH family of programs. Its structure is based upon the SIMPLE algorithm of Patankar and Spalding [16], and the discretized equations are solved by the line-by-line solution method.

Modifications are done in the present study to introduce the near-wall $k-\epsilon$ model of turbulence. In addition, the program is rewritten to be suitable to the equations in a curvilinear orthogonal co-ordinate system. Also, a subroutine is added to specify the physical properties as a function of the local temperature, (see the Appendix).

Boundary Conditions

Appropriate boundary conditions were implemented on all sides of the solution domain. At the inlet, an experimental data from Johnson [8] is used to specify the streamwise velocity and temperature distributions, and for the turbulent energy the following relation is adopted [15]:

$$k = \frac{u_{in}^2}{1000} (8.5 - 1.5 \frac{y}{H}) \tag{12}$$

The boundary condition for the streamwise velocity, u , can be stated as zero for the inner and outer walls, i.e.

$$u=0.0 \text{ at } y=0.0, \text{ and } y=H \tag{13-a}$$

is a no slip at the walls, i.e.,

$$k=0.0 \text{ at } y=0.0, \text{ and } y=H \tag{13-b}$$

while the boundary condition for ϵ is given as follows [15];

$$\epsilon_w = 2v \left(\frac{\partial \sqrt{k}}{\partial y} \right)_w^2 \tag{13-c}$$

For the fluid temperature profiles, a uniform distribution of heat flux along the duct walls is assumed as follows [8];

$$-\lambda \frac{\partial T}{\partial y} \Big|_w = \text{constant} \text{ at } y=0.0, \text{ and } y=H \tag{13-d}$$

The above boundary conditions have been used with the near-wall $k-\epsilon$ model (present model), while the wall function method is used with the standard $k-\epsilon$ model of turbulence.

RESULTS AND DISCUSSION

Validation

A schematic of the bend geometry adopted in the present study is given in Fig. 1. The value $Rc/d_{ih}=3.357$ was chosen to compare the present predictions with theoretical results by standard $k-\epsilon$ model and experimental data of Johnson [8]. Also air flow through the bend, at Reynolds number equal to 55,800, was considered for the same reason. For this bend, straight channel section were included for both upstream and downstream of bend to allow for realistic flow development. The geometric parameters characterizing the bend are given as follows;

Channel width, H	0.0899 m
Inner radius, Ri	0.2568 m
Outer radius, Ro	0.3467 m
Upstream straight section, Lu	0.4495 m
Downstream straight section, Ld	0.4495 m

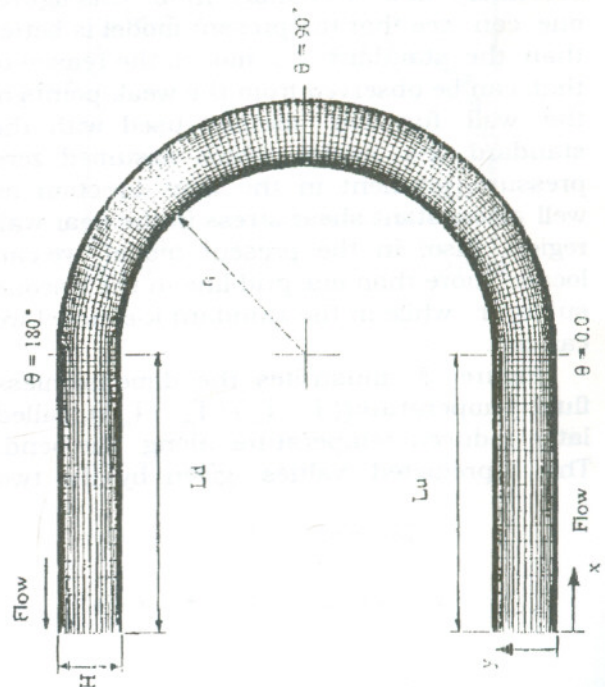


Figure 1 Two dimensional U-bend and numerical grid ($Rc/d_{ih} = 3.357$)

Figure 2 shows the dimensionless streamwise velocity u/u_{in} against the dimensionless distance y/d_h . This figure represents a comparison of both the predicted results using the present model and standard $k-\epsilon$ model of turbulence and the experimental data [8] at a location ($5d_h$ -upstream, $\theta = 0^\circ, 45^\circ, 90^\circ, 135^\circ, 180^\circ$ and $5d_h$ -downstream). Plate 2-a shows the inlet conditions for streamwise velocity in dimensionless form based on the experimental data [8] at the location $5d_h$ -upstream. These conditions are considered the boundary conditions for the present model and the standard $k-\epsilon$ model. From Plates 2-b-f one can note that there is a difference between the predicted values and experimental data along the bend. This may be due to the fact that calculations using both the present model and the standard $k-\epsilon$ model can not predict the secondary flow in three dimensional bend. For the case of two-dimensional flow the top and bottom walls is responsible for calculation of the secondary flow. Also the centrifugal force can represent a factor which influence the prediction of the secondary flow. Generally from this figure, one can see that the present model is better than the standard $k-\epsilon$ model, the reason of that can be observed from the weak points of the wall function method used with the standard $k-\epsilon$ model which assumed zero pressure gradient in the flow direction as well as constant shear stress in the near wall region. Also, in the present model we can locate more than one grid line in the viscous sublayer while in the standard $k-\epsilon$ model we can not.

Figure 3 illustrates the dimensionless fluid temperature $((T - T_w) / (T_{in} - T_w))$, called later reduced temperature along the bend. The predicted values given by the two

models and the experimental data [8] at the above locations ($5d_h$ -upstream, $\theta = 0^\circ, 45^\circ, 90^\circ, 135^\circ, 180^\circ$ and $5d_h$ -downstream) are presented for comparison. The features displayed by the temperature field at the various locations generally seem to parallel those evident in the mean streamwise velocity field at corresponding locations. In most cases, higher temperatures appear to occur in regions of low streamwise velocity, the inverse also being true. Plates 3-a and b show that the temperature profiles are nearly symmetric about the vertical line in the upstream region. The greatest departure from symmetry occurs near the outer wall where local variations in the wall heat flux are most influential. Plates 3-c-g illustrate that the reduced temperature in the present model is less than that given by the standard $k-\epsilon$ model. In general, it can be noted that the predictions of the present model showed better agreement with the experimental data than those of the standard $k-\epsilon$ model.

The calculated Nusselt numbers from the experimental data (temperature field) as well as the predicted values from the two models, along the bend are shown in Figure 4. For the numerical solution, the local Nusselt number at any point is the given by Gonsman and Ideriah [17]; (see Appendix). The distribution of Nusselt number at $\theta = 0^\circ$ seems to monotonically increase at outer wall and decreases at inner wall, and at the center of duct, the Nusselt number, Nu , is nearly flat. We can see that the average value of Nu increases as the flow passes through the bend till the half of it, ($\theta = 90^\circ$), and start to decrease at the second half. But generally the Nusselt number in the downstream is higher than that in upstream. It may be referred to the decrease of temperature difference $(T_w - T_{av})$ along the passage.

Flow and Heat Transfer Characteristics Through A U-Bend

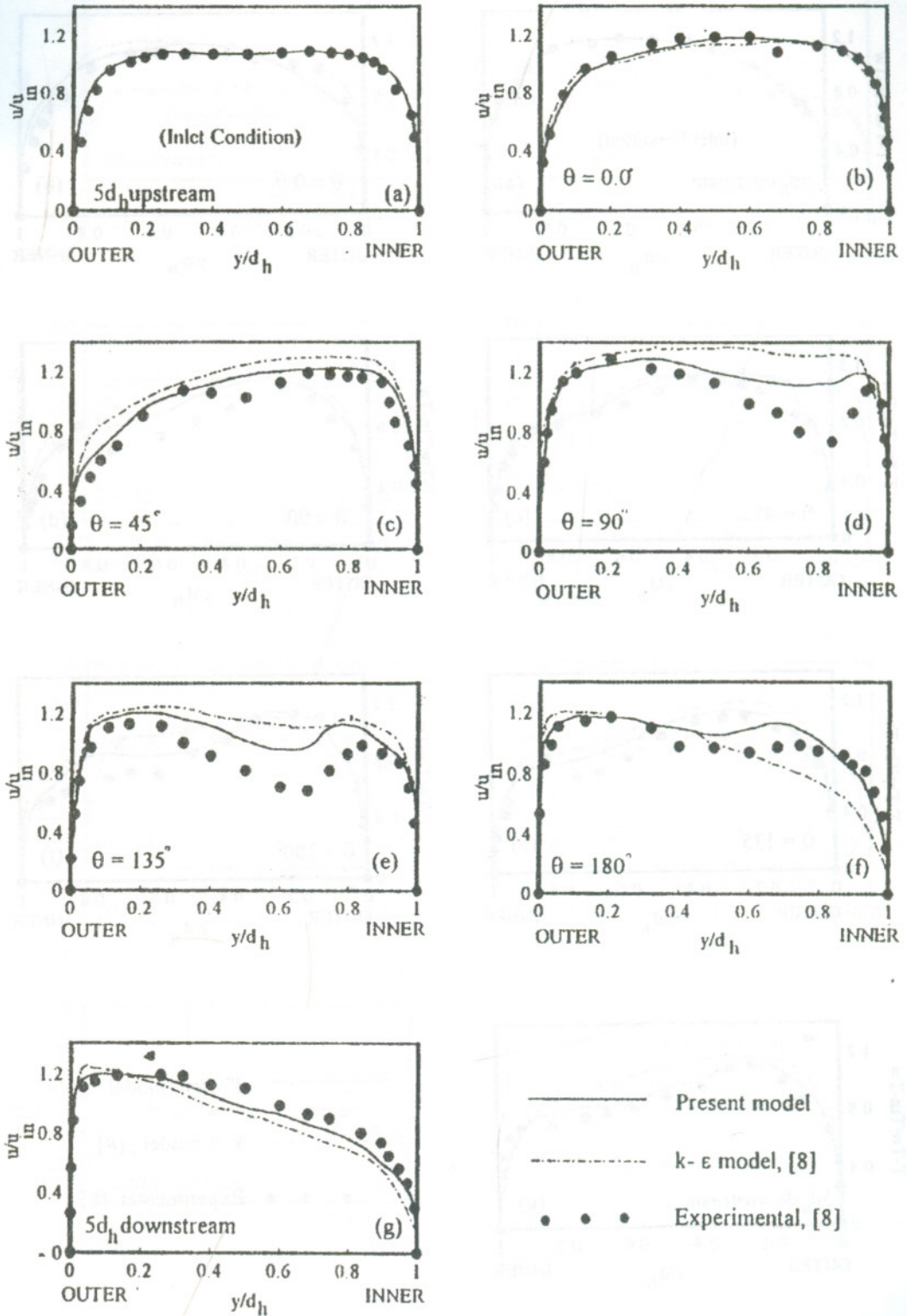


Figure 2 Mean velocity measurement for turbulent for air flow at different locations along the U-bend ($Re = 55,800$)

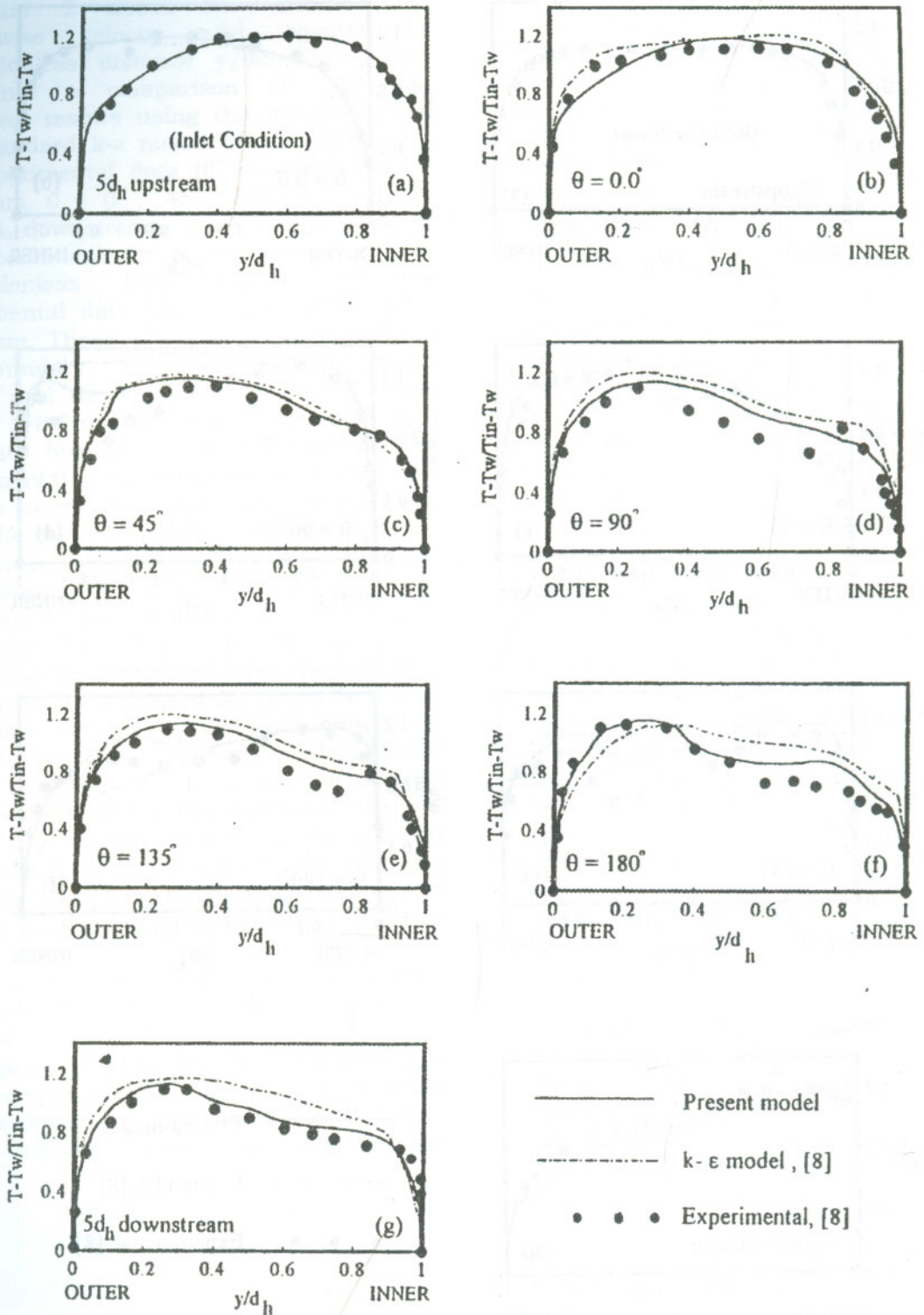


Figure 3 Reduced temperature measurements for turbulent air flow in the U-bend ($Re=555,800$)

Flow and Heat Transfer Characteristics Through A U-Bend

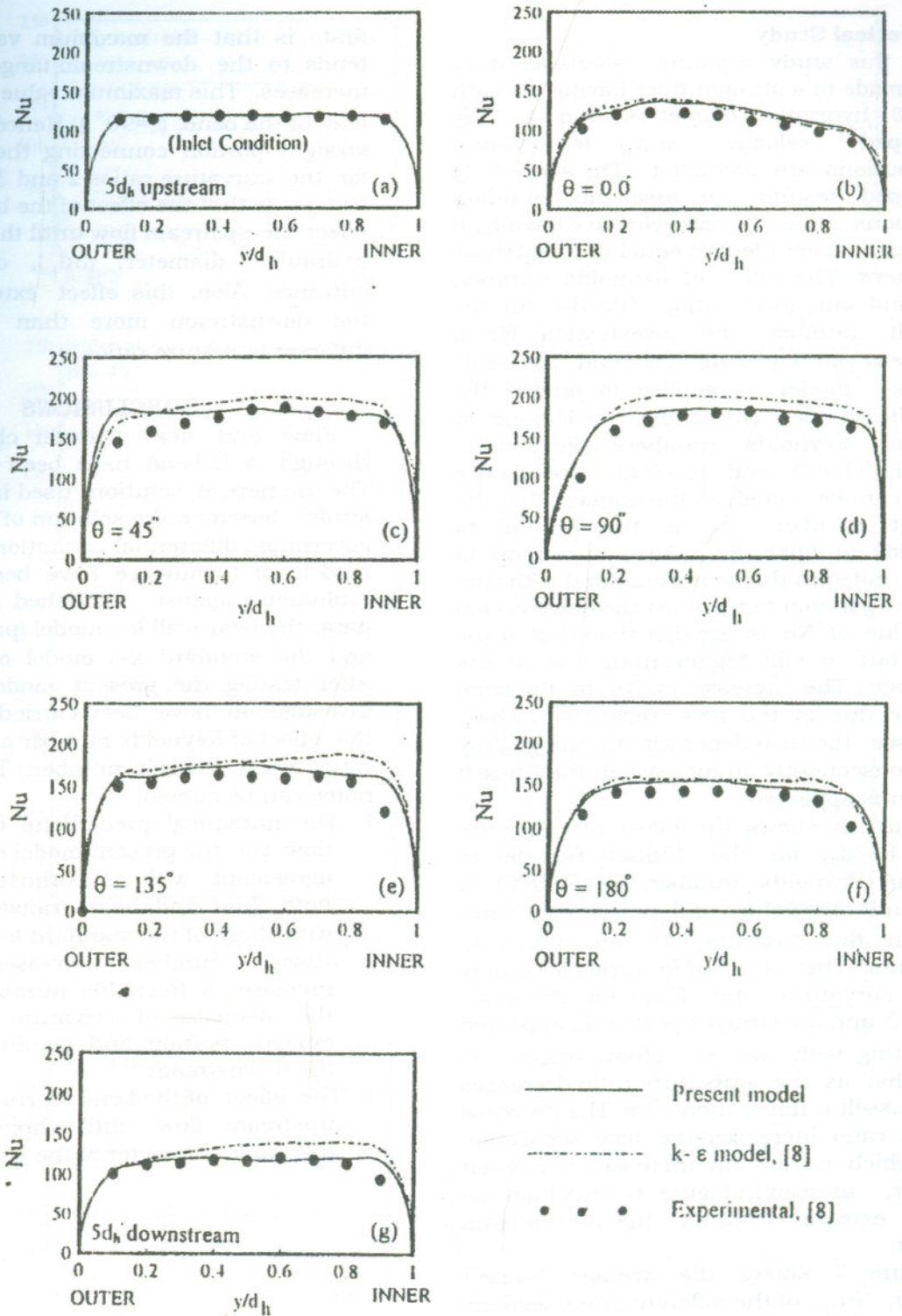


Figure 4 Nusselt number for turbulent air flow at different locations along the U-bend ($Re=55,800$)

Theoretical Study

In this study separate calculation have been made in a straight duct having a length of 50 hydraulic diameters and a fully developed velocity and temperature distributions are predicted. The above fully developed results are used as boundary conditions in a U-bend geometry having an upstream tangent length equal to 5 hydraulic diameters. The effect of Reynolds number, Re , and curvature ratio, (Rc/d_h) , on the Nusselt number are investigated for a turbulent air flow along a U-bend. The near-wall $k-\varepsilon$ model is applied to predict the Nusselt number, Nu , along the U-bend at different Reynolds numbers ($Re=10,000, 20,000, 50,000, \text{ and } 100,000$), (see Figure 5). It can be noted, as it is known, that the Nusselt number, Nu , is proportional to Reynolds number, Re . Also, an increase in Nu is noted in the bend compared with that in the upstream tangent. At the downstream the value of Nu is smaller than that at the bend but it still higher than that at the upstream. The increase of Nu in the bend may be due to the flow separation, which increases the turbulence kinetic energy [18], and consequently an increase in the Nusselt number is appeared.

Figure 6 shows the effect of curvature ratio, Rc/d_h , on the Nusselt number at constant Reynolds number, ($Re=50,000$). In this study the values of d_h and the distance between the tangents, L_t , are taken as constants. The value of Rc varies according to the curvature ratio. Thus for the ratios $Rc/d_h=2$ and 3 a straight portion is appeared connecting with two 90° -elbow ducts. It is clear that as the curvature ratio decreases the Nusselt number increases. The decrease of this ratio increases the flow separation [18], which causes an increase in Nusselt number, as seen in Figure 6. This increase of Nu extends through the downstream tangent

Figure 7 shows the average Nusselt number, Nu_{avg} , of the different cross sections along the U-bend. It is clear that the Nu_{avg} increases with the increase of Reynolds number and the decrease of curvature ratio. In this figure, one can note two features, the

first is that the maximum value of Nu_{avg} tends to the downstream tangent as the Re increases. This maximum value lies after the mid of the bend. ($\theta=90^\circ$). Hence it lies in the straight portion connecting the two elbows for the curvature ratios 2 and 3. The second feature is that the effect of the bend starts to affect the upstream flow until three times the hydraulic diameter, ($3d_h$), of the bend entrance. Also, this effect extends through the downstream more than $5d_h$ for the different curvature ratios.

CONCLUSIONS

Flow and heat transfer characteristics through a U-bend have been investigated. The numerical solution used in the present study, based on the solution of the complete governing differential equations. Two $k-\varepsilon$ models of turbulence have been tested and evaluated against published experimental data, the near-wall $k-\varepsilon$ model (present model) and the standard $k-\varepsilon$ model of turbulence. After testing the present model, theoretical investigation have been carried out to study the effect of Reynolds number and curvature ratio upon Nusselt number. The following notes can be quoted;

1. The numerical predictions for turbulent flow via the present model show a better agreement with experimental data for both fluid and heat transfer, compared with those of the standard $k-\varepsilon$ model.
2. Nusselt number increases with the increase of Reynolds number and with the decrease of curvature ratio in the curved portion and continues through the downstream.
3. The effect of the bend starts to affect the upstream flow until three times the hydraulic diameter of the bend entrance.

Flow and Heat Transfer Characteristics Through A U-Bend

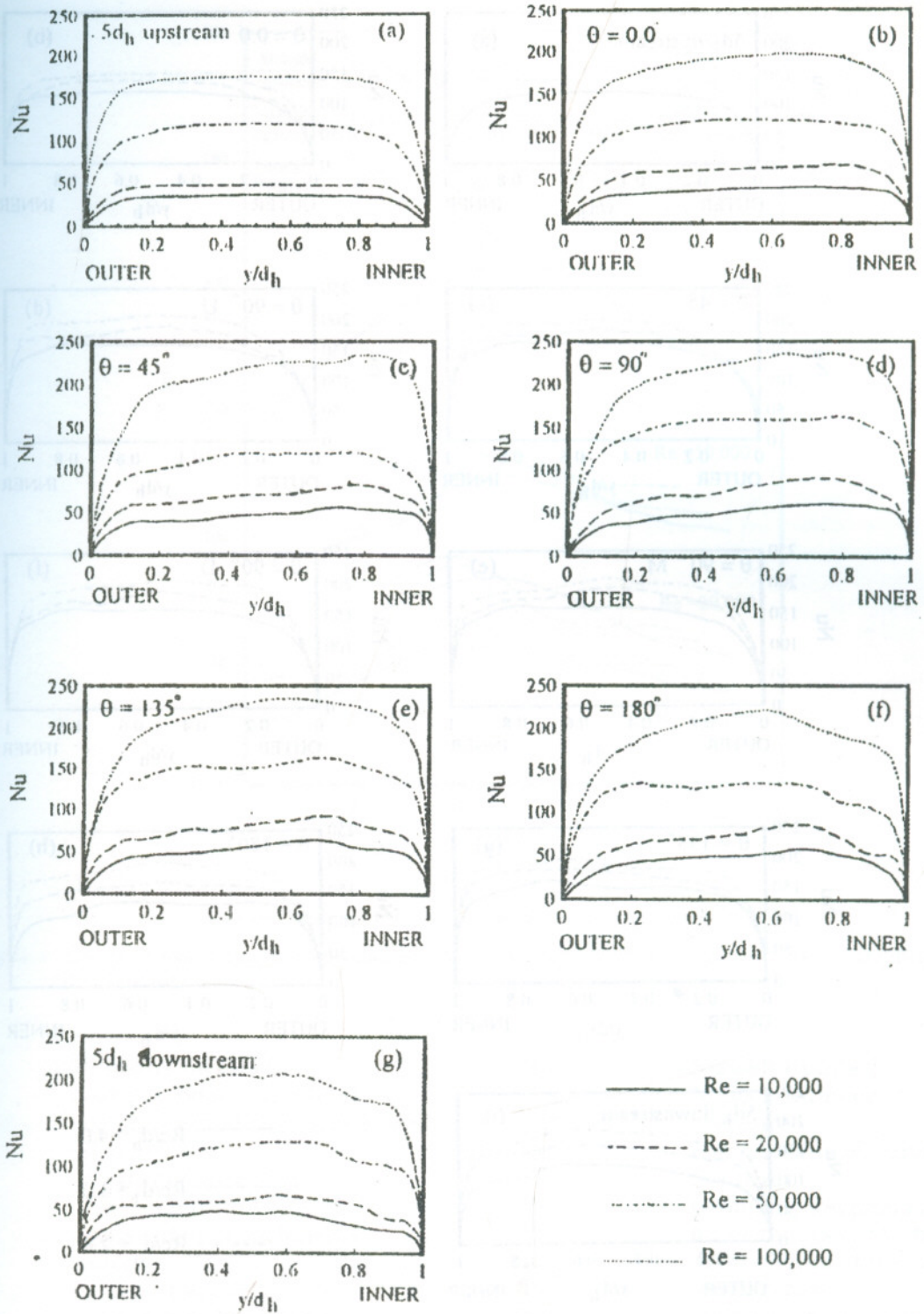


Figure 5 The predicted Nusselt number for turbulent air flow at different Reynolds number and locations along the U-bend ($Re/c_h = 4.0$)

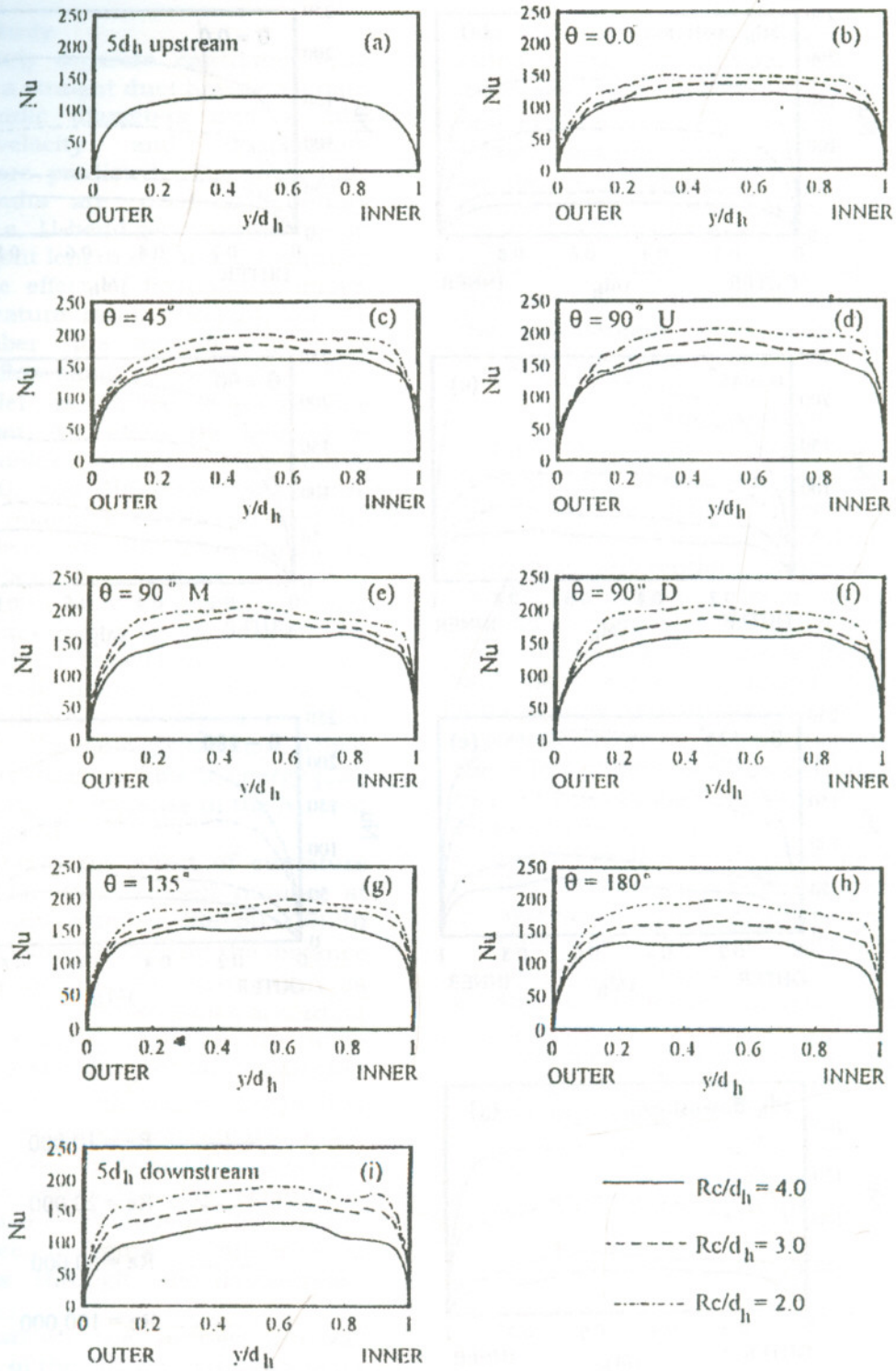


Figure 6 The predicted Nusselt number turbulent air flow at different curvature ratio (Rc/d_h) U-bend air, $Re = 50,000$

Flow and Heat Transfer Characteristics Through A U-Bend

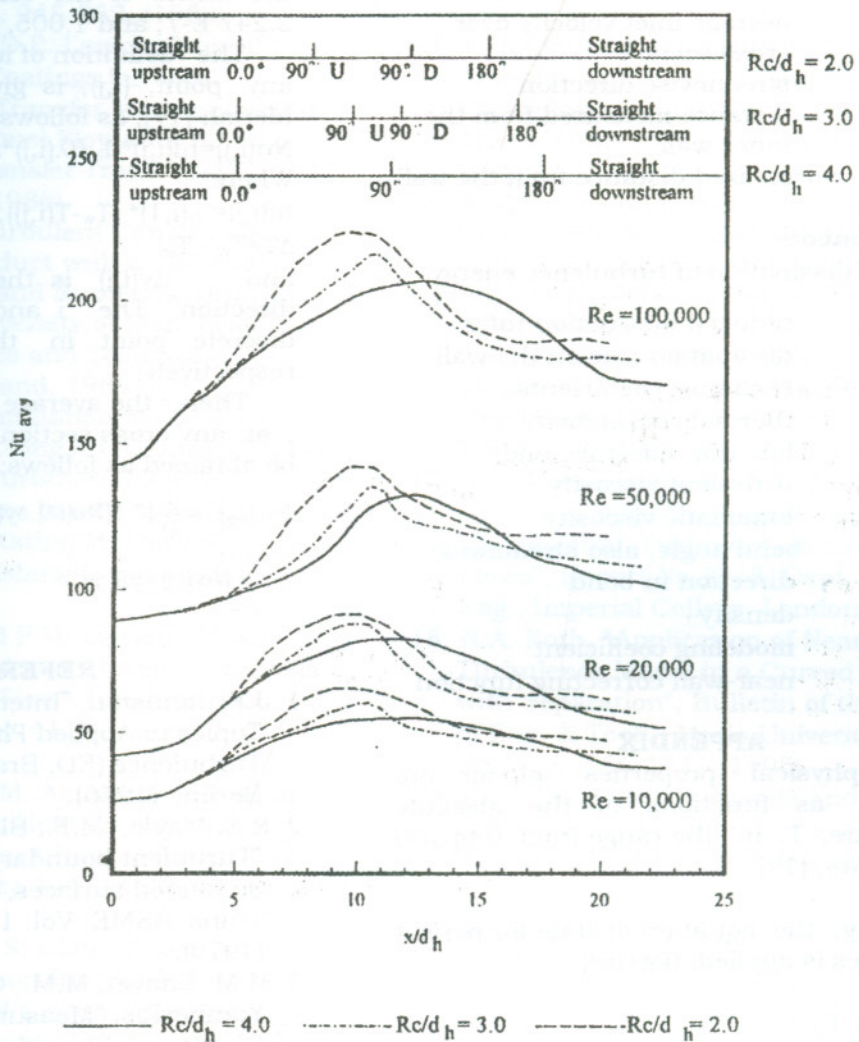


Figure 7 Average Nusselt number distributions for turbulent air flow along the U-bend at different Reynolds numbers (Re)

NOMENCLATURE

c_p	specific heat of the fluid
$C_{\epsilon 1}, C_{\epsilon 2}, C_{\mu}$	coefficients in the turbulence model
d_h	hydraulic diameter
f_{μ}	damping function
G	generation of turbulence energy
H	channel width
k	turbulence kinetic energy
L_d	downstream tangent length
L_t	distance between the tangents
L_u	upstream tangent length

Nu	Nusselt number
Nu_{avg}	Nusselt number
p	pressure
Rc	mean radius of curvature of the bend
Re_t	turbulent Reynolds number
R_i	inner radius of the bend]
R_o	outer radius of the bend
T	temperature
T_{avg}	average temperature over cross section
T_{in}	inlet temperature
T_w	wall temperature

u	local mean velocity
u _{in}	average inlet velocity over cross section
x	streamwise direction
y	distance measured from the inner wall
y ⁺	normalized distance from the wall

Greek Symbols

ϵ	rate of dissipation of turbulence energy
$\bar{\epsilon}, \epsilon^*$	reduced dissipation rates
ϵ_w	dissipation rate on the wall
$\Gamma_{e,eff}, \Gamma_{k,eff}, \Gamma_{T,eff}$	exchange coefficients
λ	thermal conductivity
μ, μ_{eff}, μ_t	laminar, effective, and turbulent viscosity
ν	kinematic viscosity
θ	bend angle, also streamwise direction in bend
ρ	density
$\sigma_k, \sigma_\epsilon, \sigma_t$	modeling coefficient
ζ	near-wall correcting function

APPENDIX

The physical properties of air are presented as functions of the absolute temperature, T, in the range from 0 to 100 °C as follows, [19]:

a-Density, the equation of state for perfect (ideal) gases is applied, (kg/m³)

$\rho = p / (Ra \cdot T)$
 where Ra is the specific gas constant for air and equal to 286.8 J/(kg.K),
 and p is the air pressure, N/m²

b-Dynamic viscosity, μ , (kg/m.s)
 $\mu = (aT^2 + bT + c) \cdot 10^{-5}$
 the values of the constants a, b, and c are -1.0719 E-7, 5.247E-3, and 0.367, respectively.

c-Thermal conductivity, λ (W/m.K)
 $\lambda = a_1 T^2 + b_1 T + c_1$
 the values of the constants a₁, b₁, and c₁ are -3.1622 E-8, 8.6818E-3, and 0.003549, respectively

d-Specific heat, cp, (kJ/kg.K)
 $cp = a_2 T^2 + c_2$

the values of the constants a₂, and c₂ are 2.247 E-7, and 1.005, respectively

The definition of local Nusselt number at any point, (i,j), is given by Gonsman and Ideriah [17], as follows;

$Nu(i,j) = hf(i,j) \cdot d_h / (\lambda(i,j) \cdot \Delta T)$ (A-1)

Where
 $hf(i,j) = \lambda(i,1) \cdot (T_w - T(i,j)) / \Delta y(i,j)$ (A-2)

$\Delta T = T_w - T_{in}$ (A-3)

and $\Delta y(i,j)$ is the increment in the y-direction. The i and j are the numerical discrete point in the x and y directions respectively.

Then, the average Nusselt number, Nu_{avg}, at any cross section along the bend, x, can be obtained as follows;

$Nu_{avg}|_i = \frac{1}{H} \{0.5[Nu(i,1) \cdot \Delta y(i,1) + Nu(i,n) \cdot \Delta y(i,n)] + \sum_{j=2}^{j=n-1} Nu(i,j) \cdot \Delta y(i,j)\}$ (A-4)

REFERENCES

1. J.P. Johnston, "Internal flows, Chap. 3 in Topics in Applied Physics", Vol. 12, Turbulence (ED. Bradshaw, P.) Springer, Berlin, (1976).
2. R.E. Mayle, M.F., Blair and F.C. Kopper, "Turbulent boundary layer heat transfer on curved surfaces, J. Heat transfer Trans. ASME, Vol. 101, pp. 521-530, (1979).
3. M.M. Enayet, M.M., Gibson and M. Yianneskis, "Measurements of Turbulent Developing Flow in a Moderately Curved Square Duct, Int. J. Heat Fluid Flow, Vol. 3, pp. 221-229, (1982).
4. A.M.K.P. Taylor, J.H. Whitelaw, and M. Yianneskis, "Curved Ducs with Strong Secondary Motion: Velocity Measurements of Developing Laminar and Turbulent Flow, J. Fluids Eng. Trans. ASME, Vol. 104, pp. 350-359, (1982).
5. J.A.C. Humphrey, J.H. Whitelaw and G. Yee, "Turbulent Flow in a Square Duct With Strong Curvature, J. Fluid Mech., Vol. 103, pp. 443-463, (1981).
6. N.A. Kotb, M.R. Mokhtarzadeh and A.J. Ward, "A Numerical Study of Laminar and Turbulent Flows in a Two-Dimensional Bend with or Without a Guide Vane", Int,

- J, for Numerical Methods in Engineering, Vol. 26, No. 5, pp. 245-262, (1988).
7. D.E. Metzger and D.E. Larson, "Use of Melting Surface Coatings for Local Convection Heat Transfer Measurement in Rectangular Channel Flow with 90 Deg. turns", J. Heat transfer Trans. ASME, Vol. 108, pp. 48-54, (1986).
 8. R.W. Johnson, "Turbulent Convecting Flow in a square duct with a 180 ° bend, an Experimental and Numerical Study", Ph.D. Thesis, University of Manchester Institute of Science and Technology, Manchester, England, 1984.
 9. R.W. Johnson, "Simulation of Local Nusselt Number Using an Algebraic Stress Model (ASM) for Turbulent Flow in a Square 180 ° degree bend", Transport Phenomena in Rotating Machinery, Hemisphere Publishing Corporation, pp. 313-329, (1988).
 10. C.R. Hedlund and P.M. Ligrani, "Heat Transfer in Curved and Straight Channels with Transitional Flow", Int. J. of Heat Mass Transfer, Vol. 41, No. 3, pp. 563-573, (1998).
 11. K.C. Chence and M. Akiyama, "Laminar Forced Convection Heat Transfer in Curved Rectangular Channels", Int. J. of Heat Mass Transfer, Vol. 13, No. 1, pp. 471-490, (1970).
 12. P.M. Ligrani and S. Choi, "Effect of Deen Vortex Pairs on Surface Heat Transfer in Curved Channel Flow", Int. J. of Heat Mass Transfer, Vol. 39, No. 1, pp. 27-37, (1996).
 13. P.M. Ligrani and S. Choi "Mixed Convection in Straight and Curved Channel with Buoyancy Orthogonal to the Forced Flow", Int. J. of Heat Mass Transfer, Vol. 39, No. 12, pp. 2475-2484, 1996.
 14. V. Kadambi E.K. Levy and S. Neti, "Heat Transfer and Pressure Drop in a Helically Coiled Rectangular Duct", J. Heat transfer Trans. ASME, Vol. 108, pp. 343-349, (1986).
 15. R.M.C. So and A. Sarkar, "Turbulent Couette Flows-An Assessment of Ten Near-Wall Two-Equation models", Report No ASU/TFML-94-3, (1994).
 16. S.V. Patankar and D.B. Spalding, "A Calculation Procedure for Heat, Mass and Momentum Transfer in Three-Dimensional Parabolic Flows, Int. J. Heat Transfer, Vol. 15, pp. 1787-1806, (1972).
 17. A.D. Gonsman and F.J.K. Ideriah, "A General Computer Program for Two-Dimensional, Turbulent, Recirculating Flows", Report No.12/8, Dept. of Mech. Eng., Imperial College, London, (1976).
 18. N.A. Kotb, "Application of Near-Wall Turbulence Model in a Curved Channel with Separation", Bulletin of the Faculty of Eng. & Tech., Minia University, Vol. 14, No 1, pp. 156-171, (1995)..
 19. R.C. Reid, J.M., Prausnitz and T.K. Sherwood." The Properties of gases and liquids", Third Ed., McGraw-Hill, (1977).

Received November 21, 1998
Accepted March 6, 1999

خصائص السريان وانتقال الحرارة خلال منحنى على شكل حرف U

نبيل قطب، إبراهيم محمود المغازي ، عادل حجازي و محمد عطية

قسم هندسة القوى الميكانيكية - جامعة المنيا

ملخص البحث

تناول هذه الدراسة خصائص السريان وانتقال الحرارة خلال منحنى على شكل حرف U حيث تم حل المعادلات التفاضلية الحاكمة للسريان بالطرق العددية مستخدما نموذج الاضطراب $k-\epsilon$ مع التصحيح قرب الجدار (النموذج الحالي) وقورنت النتائج مع نتائج نموذج الاضطراب القياسي $k-\epsilon$ على اساس النتائج العملية لسريان الهواء خلال قناة منحنية على شكل حرف U ذات مقطع رباعي الشكل وقد تبين تطابق نتائج النموذج الحالي مع النتائج العملية أفضل من تطابق نتائج النموذج القياسي ثم استخدم النموذج الحالي في دراسة تأثير كل من درجة الانحناء للقناة ورقم رينولدز على رقم ناسلت (معدل انتقال الحرارة) حيث أظهرت هذه الدراسة أن زيادة رقم رينولدز وتناقص درجة الانحناء يزيد من رقم ناسلت في الجزء المنحنى وتستمر هذه الزيادة خلال المماس الخلفية للقناة.